Downstream sequence-dependent RNA cleavage and pausing by RNA polymerase I

Received for publication, October 3, 2019, and in revised form, December 3, 2019 Published, Papers in Press, December 16, 2019, DOI 10.1074/jbc.RA119.011354

Catherine E. Scull[‡], Andrew M. Clarke[‡], Aaron L. Lucius[§], and David Alan Schneider[‡1]

From the Departments of [‡]Biochemistry and Molecular Genetics and [§]Chemistry, University of Alabama at Birmingham, Birmingham, Alabama 35294

Edited by Craig E. Cameron

The sequence of the DNA template has long been thought to influence the rate of transcription by DNA-dependent RNA polymerases, but the influence of DNA sequence on transcription elongation properties of eukaryotic RNA polymerase I (Pol I) from *Saccharomyces cerevisiae* has not been defined. In this study, we observe changes in dinucleotide production, transcription elongation complex stability, and Pol I pausing *in vitro* in response to downstream DNA. *In vitro* studies demonstrate that AT-rich downstream DNA enhances pausing by Pol I and inhibits Pol I nucleolytic cleavage activity. Analysis of Pol I native elongating transcript sequencing data in *Saccharomyces cerevisiae* suggests that these downstream sequence elements influence Pol I *in vivo*. Native elongating transcript sequencing studies reveal that Pol I occupancy increases as downstream AT content increases and decreases as downstream GC content increases. Collectively, these data demonstrate that the downstream DNA sequence directly impacts the kinetics of transcription elongation prior to the sequence entering the active site of Pol I both *in vivo* and *in vitro*.

DNA-dependent RNA polymerases transcribe DNA to produce RNA and, thus, are responsible for all genetic expression in living organisms. It has long been appreciated that the rate of transcription elongation for all three nuclear eukaryotic RNA polymerases (Pols)[2] is dynamic in nature (1). The dynamic nature of polymerase transcription is critical for correct splicing of mRNA genes by Pol II (1) and for correct folding and cotranscriptional modification of Pol I–synthesized rRNA (2). *In vitro* and *in vivo* studies have shown that many alterations in transcription elongation rate are protein-mediated and controlled by both activating and repressing transcription elongation factors and histone modifications (1, 3–5). It is less clear, however, whether the template DNA sequence itself is a driver of the *in vivo* diversity of the transcription rate. *In vitro* studies suggest that RNAP from *Escherichia coli* exhibits a heterogeneous transcription elongation rate in the absence of transcription elongation factors (6, 7). Further *in vitro* studies characterizing transcription termination have shown that Pol transcription through A-rich template DNA tracts results in destabilization of the transcription elongation complex through accumulation of U:dA base pairs in the RNA:DNA hybrid. This destabilization is required for transcription termination (8, 9). A study published recently by our laboratory demonstrated that specific DNA template sequences affect Pol I transcription elongation in a nucleotide concentration– dependent manner *in vitro* and suggested that Pol I is sensitive to DNA sequence elements *in vivo* (9). Specifically, native elongating transcript sequencing (NET-seq) adapted for *Saccharomyces cerevisiae* (yeast) Pol I elucidated that Pol I occupancy on ribosomal DNA is heterogeneous, which could imply that DNA sequence impacts pausing and Pol I elongation rate *in vivo* (9). However, in the presence of other transcription factors and chromatin modifications, it is difficult to say whether the heterogeneity of Pol I occupancy observed *in vivo* is a direct result of DNA sequence or whether it is mediated by other factors. This study also did not identify consensus DNA sequences that induced pausing *in vivo* (9).

There has been work done regarding the impact of upstream DNA sequence on both prokaryotic Pol and eukaryotic RNA polymerase II activity (10, 11) as well as on the influence of the identity of the incorporated nucleotide during nucleotide addition (12, 13), and some studies have also been done to probe the downstream sequence effects on transcription elongation complex properties (14–24). There have been no previous studies, however, analyzing downstream sequence effects on RNA polymerase I. As ribosome biogenesis is tightly coupled to the rate of transcription elongation (2, 25, 26) and implicated in a number of diseases (27–29), it is critical to gain a complete understanding of the mechanisms that control transcription by RNA polymerase I.

In this study, we characterize the influence of downstream DNA sequence on the transcription elongation properties of Pol I from yeast both *in vitro* and *in vivo*. *In vitro* analyses using a scaffold-based DNA template reveal that yeast Pol I pauses at a higher frequency in the context of increased AT downstream sequence, similar to previous observations with Pol II (15). Interestingly, we observed that AT-rich downstream sequences also repress RNA cleavage by Pol I. Through mutational analy-

This study was supported by National Institutes of Health Grant GM084946 (to D. A. S.) and T32 Grant GM008111 (to C. E. S.). This work was also funded by National Science Foundation Grant MCB-1817749 (to A. L. L. and D. A. S.). The authors declare that they have no conflicts of interest with the contents of this article. The content is solely the responsibility of the authors and does not necessarily represent the official views of the National Institutes of Health.

This article contains Figs. S1–S4.

[1] To whom correspondence should be addressed. Tel.: 205-934-4781; E-mail: dschneid@uab.edu.

[2] The abbreviations used are: Pol, RNA polymerase; NET-seq, native elongating transcript sequencing; ETS, externally transcribed sequence; ITS, internally transcribed sequence.

© 2020 Scull et al. Published under exclusive license by The American Society for Biochemistry and Molecular Biology, Inc.

Downloaded from http://www.jbc.org/ at Univ of Alabama Birmingham, Lister Hill Library of the Health Sciences on April 24, 2020

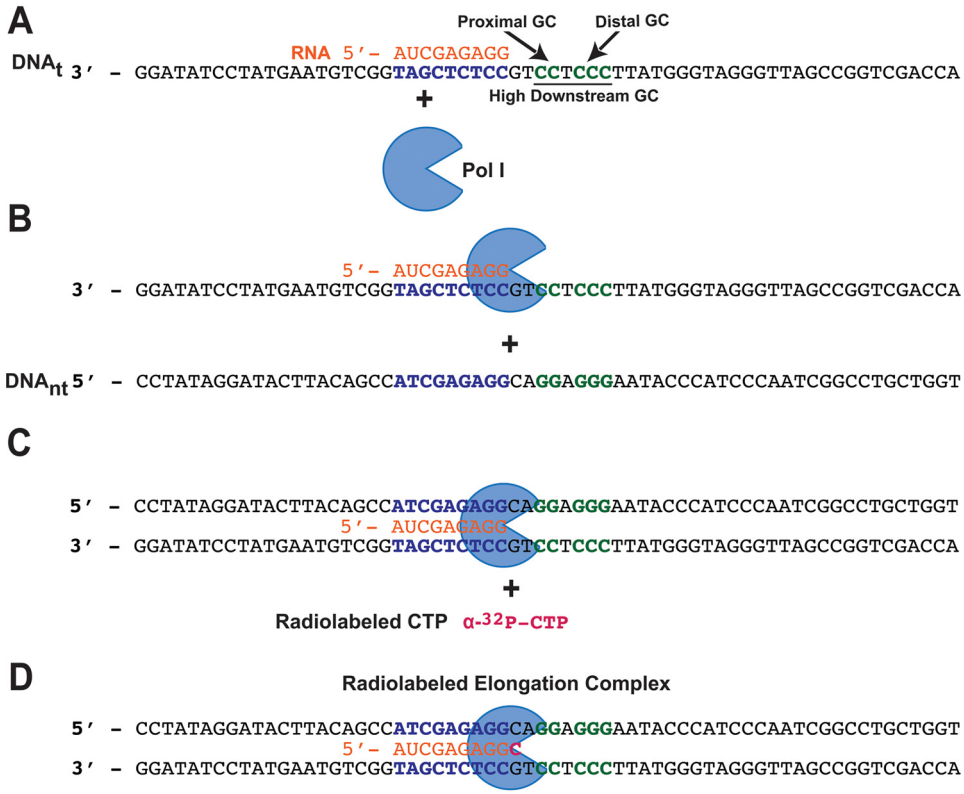

Figure 1. Construction of the synthetic Pol I transcription elongation complex. *A* and *B*, Pol I elongation complexes are constructed by first incubating Pol I with a preannealed RNA:DNA hybrid (*A*), and then nontemplate DNA is added to form the elongation complex bubble (*B*). Importantly, the actual size of the bubble has not been determined for Pol I with these templates, thus we do not depict annealing of the upstream or downstream regions of the DNA. However, we have established previously that the nontemplate strand does impact transcription elongation by Pol I; thus, it is likely annealed to the template DNA, we simply cannot say how far upstream and downstream annealing occurs (31). *C* and *D*, radiolabeled [α-^{32}P]CTP is added to solution (*C*) to form a radiolabeled 10-mer RNA species (*D*).

sis, two distinct regions of Pol I that are structurally close to the downstream DNA were altered to probe whether they sensitized the polymerase to downstream DNA sequence. Loss of sensitivity to distal AT-rich regions was observed when the gene that encodes the nonessential subunit responsible for proofreading and RNA cleavage, subunit A12.2 (A12), of Pol I was deleted. Further, NET-seq revealed that this downstream DNA sequence effect is conserved *in vivo*. Together, these findings demonstrate that Pol I physically interrogates the downstream DNA sequence (at least in part through the A12 subunit) and that these sequence elements directly influence rRNA synthesis both *in vivo* and *in vitro*.

Results

Single-nucleotide addition experiments with an AT-rich downstream sequence alter Pol I pause escape and dinucleotide production

Our laboratory has previously published detailed characterizations of Pol I transcription elongation using a synthetic, 56-nucleotide-long DNA transcription template containing high-GC downstream DNA (30–32). In these previously published experiments, we built elongation complexes by incubating Pol I with a preannealed RNA:DNA$_{template}$ hybrid (Fig. 1*A*). We then added the nontemplate strand to form the elongation complex bubble (Fig. 1*B*). We added radioactive [α-^{32}P]CTP (Fig. 1*C*) to produce a radiolabeled elongation complex (Fig. 1*D*). A GC dinucleotide was produced during labeling, but this reaction was quenched with excess EDTA (to chelate the Mg^{2+} cofactor and inhibit Pol I RNA elongation and cleavage) prior to elongation complex mixing with ATP. Because this reaction was quenched prior to mixing with ATP, the signal of the GC species was constant throughout all time courses (Fig. 2*B*). After the radiolabeled elongation complex was synthesized, saturating [ATP] was added to extend the radiolabeled 10-mer RNA by one nucleotide to produce an 11-mer RNA species over time under rapid mixing conditions in a chemical quenched-flow instrument (Fig. 2*B*). The 11-mer species was subsequently cleaved by the intrinsic cleavage activity of Pol I to produce an unlabeled 9-mer species and a radiolabeled dinucleotide species (denoted as CA) (Fig. 2*B*). Heparin was included in reactions to ensure single-turnover conditions. To test the impact of downstream DNA sequence on nucleotide addition by Pol I, we conducted single-nucleotide addition experiments using two DNA templates: one containing a high downstream GC sequence (high GC) and a second with high downstream AT (high AT) content (Fig. 2*A*).

In this study, the upstream DNA and RNA remained identical between the high GC and high AT templates, and the nucleotide added to the RNA chain (AMP) was also identical. For the high AT template, the GC downstream nucleotides (Fig. 2*A*, *green*) were switched to AT nucleotides (Fig. 2*A*, *yellow*). The sole difference between the previously reported experiments described above and the high AT template data reported here is the downstream DNA context in which the single AMP nucle-

Downloaded from http://www.jbc.org/ at Univ of Alabama Birmingham, Lister Hill Library of the Health Sciences on April 24, 2020

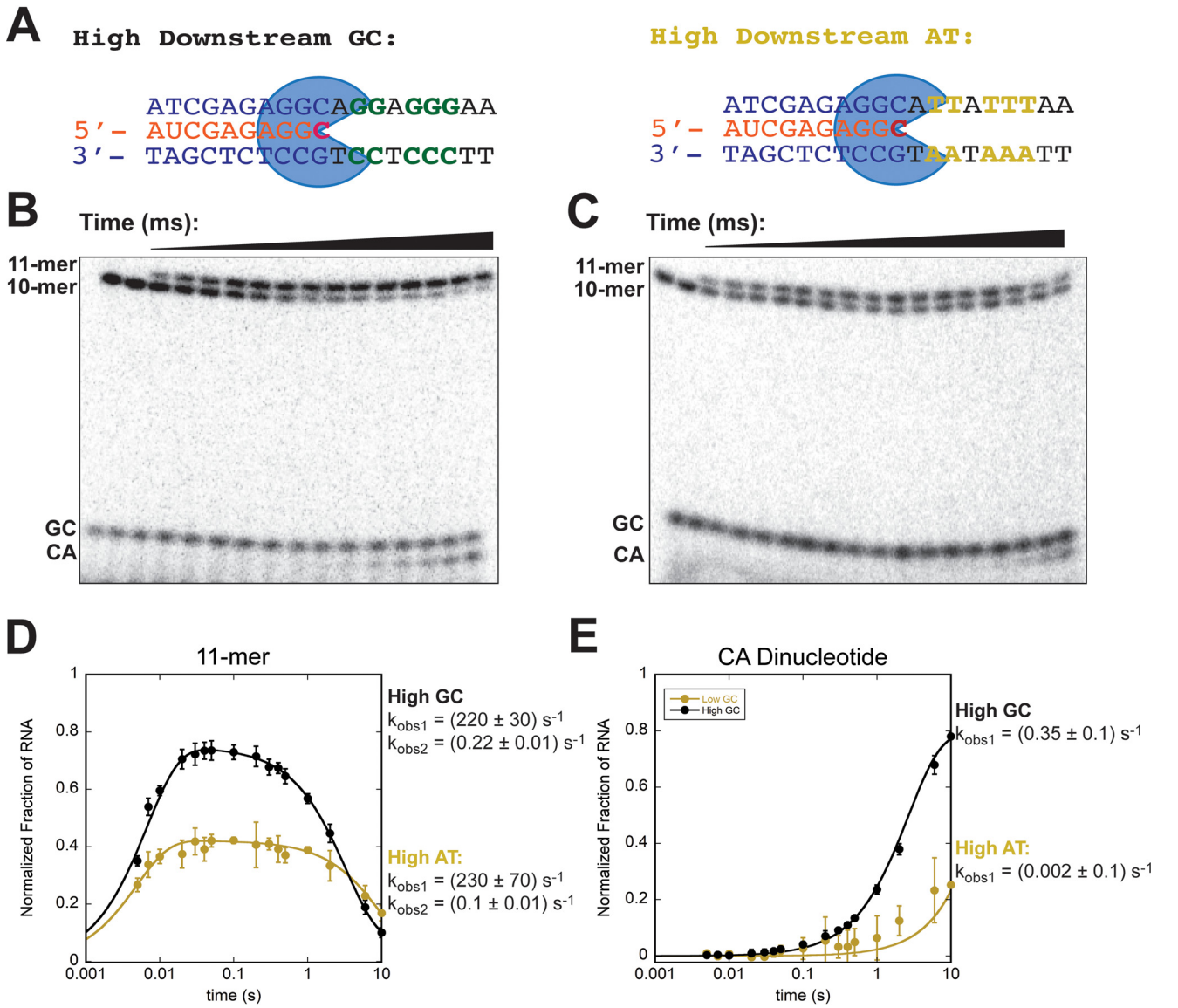

Figure 2. AT-rich downstream DNA results in suppression of 10-mer extension and decreased RNA cleavage. *A*, single-nucleotide addition by RNA polymerase I (*light blue Pac-Man*) was measured with polymerases on templates with high downstream GC content and high downstream AT content. *B* and *C*, 28% denaturing urea PAGE gels reveal an increase in 10-mer species throughout the high AT time course (*C*) compared with high GC (*B*), concurrent with a decrease in CA dinucleotide production throughout the high AT time course (*C*) compared with high GC (*B*). *D* and *E*, quantification of high GC (*black*) and high AT (*gold*) time courses for both the 11-mer (*D*) and the CA dinucleotide species (*E*) (n3, error bars represent standard deviation of the mean). Data were fit to the sum of two exponentials for the 11-mer species and a single exponential for the CA dinucleotide species.

otide is added. Two clear differences were observed when transcription was executed with the high AT DNA template compared with the high GC template. First, there was a decrease in the radioactive signal amplitude of the 11-mer species relative to the 10-mer species for the high AT template (Fig. 2*C*) compared with the high GC template (Fig. 2*B*). This was a result of persistent abundance of 10-mer species signal over the length of the time course for the high AT template (Fig. 2*C*) relative to the high GC template (Fig. 2*B*). Second, there was a decrease in the radioactive signal amplitude of CA dinucleotide produced from cleavage of the 11-mer species with the AT template (Fig. 2*C*) compared with the high GC Template (Fig. 2*B*).

Model-independent fitting of the high AT and high GC time courses displayed a decreased observed rate constant (11-mer k_{obs2} and CA dinucleotide k_{obs1}) for dinucleotide production for the high AT template compared with the high GC template (Fig. 2, *D* and *E*, respectively). Interestingly, the rate constant describing nucleotide addition (k_{obs1}) was not statistically significantly different for the high AT template (Fig. 2*D*, *gold*) compared with the high GC template (Fig. 2*D*, *black*), suggesting that the persistent 10-mer species and the extended 11-mer species may be resultant of two distinct populations of polymerases. Importantly, it is unclear from these studies whether the polymerases that did not extend the 10-mer RNA are actively engaged in the elongation complex or whether they are terminated or arrested on the DNA. Collectively, these observations suggest that downstream DNA interacts with the polymerase and alters nucleotide addition and cleavage activity by RNA polymerase I.

Downloaded from http://www.jbc.org/ at Univ of Alabama Birmingham, Lister Hill Library of the Health Sciences on April 24, 2020

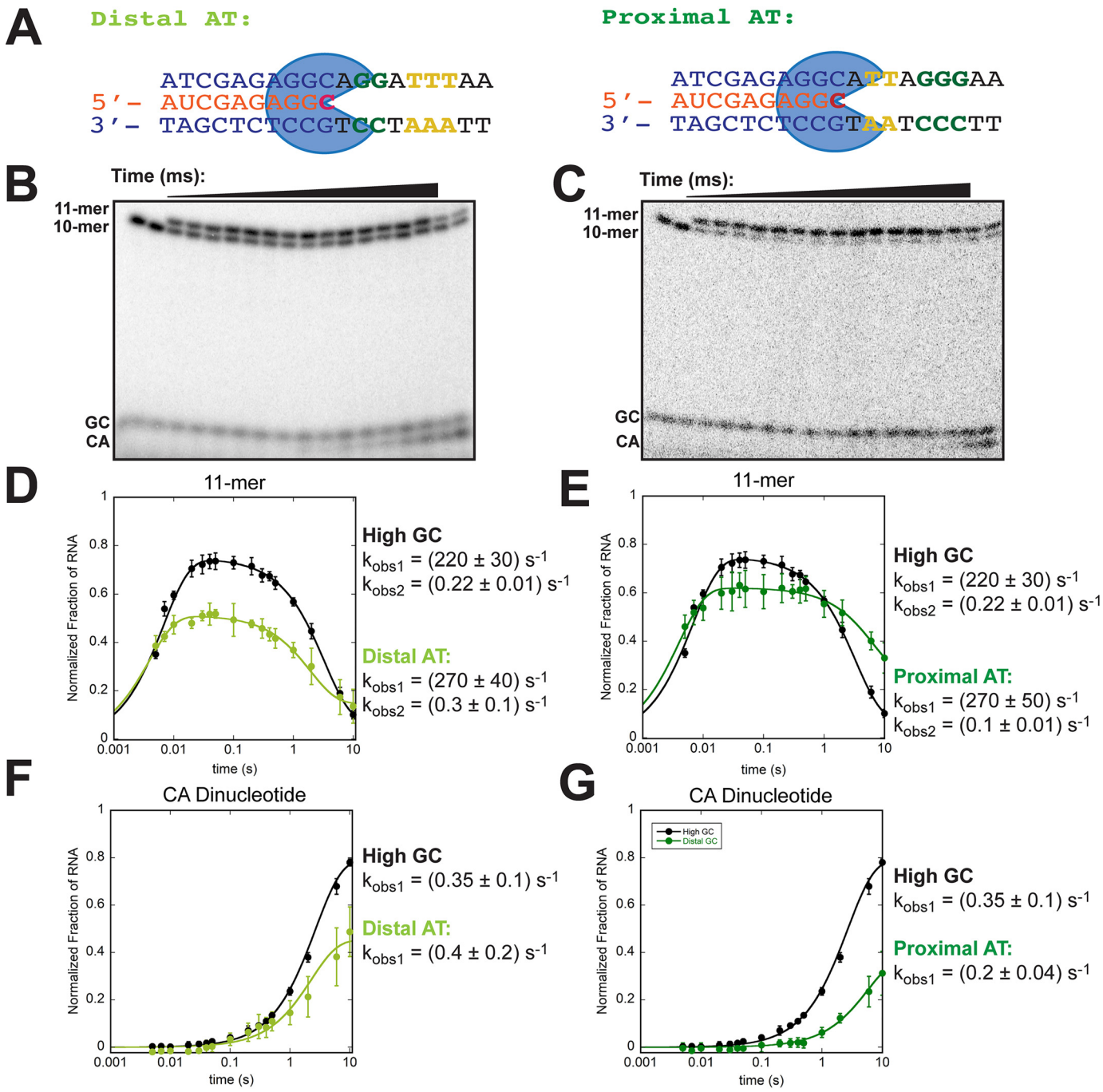

Figure 3. The distal AT region drives 11-mer suppression, and the proximal AT region drives RNA cleavage deficiency. *A*, single-nucleotide addition by RNA polymerase I (*light blue Pac-Man*) was measured with polymerases on templates with proximal and distal high downstream AT content. *B* and *C*, 28% denaturing urea PAGE gels reveal an increase in 10-mer species throughout the distal AT time course (*B*), whereas a decrease in CA dinucleotide production is noted in the proximal AT time course (*C*). *D* and *E*, quantification of Distal AT (*D* and *F*, *light green*) and Proximal AT (*E* and *G*, *dark green*) time courses compared with High GC (*black*) time courses for both the 11-mer (*D* and *E*) and the CA dinucleotide species (*F* and *G*) (n 3, error bars represent standard deviation of the mean). Data were fit to the sum of two exponentials for the 11-mer species (*D* and *E*) and a single exponential for the CA dinucleotide species (*F* and *G*).

Distal and proximal GC-rich downstream sequences have unique effects on dinucleotide production and 10-mer abundance, respectively

To probe which region of the downstream AT-rich sequence is responsible for perturbing Pol I activity in the high AT template used in Fig. 2, we altered the +2 to +3 nucleotides to AT in one template (which will be referred to as proximal AT, *dark green*) and the +5 to +7 GC-rich sequence to AT in a second template (denoted as distal AT, *light green*) (Fig. 3*A*). The distal AT template increased the radioactive signal abundance of the 10-mer species compared with the high GC template 10-mer species over the length of the time courses (compare Fig. 3*B* with Fig. 2*B*). The distal AT template also caused a slight reduction in the radioactive signal amplitude of the dinucleotide species compared with the high GC template (compare Fig. 3*B* with Fig. 2*B*). The proximal AT template had the same relative

Downloaded from http://www.jbc.org/ at Univ of Alabama Birmingham, Lister Hill Library of the Health Sciences on April 24, 2020

amount of 10-mer compared with the high GC template but resulted in a decrease in abundance of the cleaved CA dinucleotide species (compare Fig. 3*C* with Fig. 2*B*). Model-independent fitting of the dinucleotide CA species to a single exponential function revealed that the observed rate constants for the proximal AT template were significantly slower than those of the high GC template (Fig. 2*G*). Further, although the amplitude of cleaved product is lower for the distal AT template, the rate constant describing cleavage is within error of the high GC template (Fig. 3*F*, k_{obs1}).

Collectively, these observations suggest that the +2 to +3 AT sequence is primarily responsible for impairing nucleolytic cleavage by Pol I, whereas the +5 to +7 AT sequence drives the observed amplitude suppression of the 11-mer species. This initially seemed surprising, as one might expect the +2 to +3 region to have a greater direct effect on stability of the transcription elongation complex (if the polymerase falls out of the elongation complex) or backtracking and arrest of the polymerase (if the polymerase is still engaged but inactive) than the +5 to +7 region, as it is closer to the active site. These observations are, however, consistent with previously observed downstream sequence effects of downstream AT-rich regions on human Pol II (15) and *E. coli* RNAP (16). Structural studies of the downstream DNA transcribed by Pol I suggest that the +5 to +7 region of the DNA is potentially annealed (33), which implies that one or more domains of the polymerase may be interacting with double-stranded downstream DNA in a sequence-dependent manner.

The high AT and proximal GC templates have a small destabilizing effect on elongation complex stability compared with the distal GC and high GC templates

Although backtracking and arrest are known to be linked to a decrease in elongation complex stability (9), it is important to distinguish whether the persistent 10-mer species in high AT and distal AT template time courses is the result of either halted or disengaged polymerases. In these elongation complex stability experiments, radiolabeled elongation complexes are assembled (exactly as for single-nucleotide addition assays described previously) and mixed with RNase A at 40 mM KCl (the same concentration of salt as used in single-nucleotide addition assays) (34). Elongation complexes that fell apart released free RNA that was cleaved by RNase A to produce a 7-mer species, whereas intact elongation complexes protected the RNA from RNase A activity and resulted in an uncleaved 10-mer RNA species (Fig. 4*A*).

We executed elongation complex stability experiments with all four DNA templates (high GC, high AT, proximal AT, and distal AT) (Fig. 4*B*). A slight loss of elongation complex stability was observed for all templates on the timescale where single-nucleotide addition assays are executed, as noted by RNase-dependent cleavage of the 10-mer RNA to a 7-mer species (Fig. 4*B*). A similar trend was observed for the decreased elongation complex stability and persistence of the 10-mer species, as the elongation complexes with high AT (Fig. 4*C*, *gold*) and distal AT (Fig. 4*E*, *light green*) templates appeared to be the least stable, although most time points were still within error of elongation complexes bound to the high GC template (Fig. 4, *C–E*, *black*). Importantly, the difference in elongation complex stability observed between the high AT, distal AT, and high GC templates cannot account for the large population of 10-mer species observed throughout single-nucleotide transcription time courses with high AT and distal AT templates (Figs. 2*C* and 3*B*). For example, elongation complexes with the high AT template were ~10% less stable than with the high GC template (Fig. 4*C*), but the amplitude change for the high AT template compared with the high GC template was ~35% (Fig. 2*D*). These elongation complex stability data suggest that, although a small fraction of the increased 10-mer species can be accounted for by elongation complex dissociation, the majority of the population of polymerases remain engaged and are either arrested or stably paused on the DNA.

Mutations of potential downstream interacting regions suggest that both the trigger loop and the A12 subunit of Pol I contribute to downstream sequence effects

We tested the AT-rich template on previously described Pol I mutants that have been implicated in Pol I backtracking and arrest (the A12.2 subunit) (35) and that have been proposed to contact the downstream DNA in conserved regions of Pol II (the trigger loop domain of the A190 subunit) (15, 36). The A12.2 subunit directly contributes to transcription elongation complex stability and backtrack recovery (32, 34, 35). We tested whether Pol I lacking the entire A12 subunit would be more or less likely to arrest as a 10-mer species in single-nucleotide transcription elongation experiments. In these single-nucleotide transcription experiments on the AT-rich template, there was no observed suppression of the 11-mer *versus* 10-mer ratio with the ΔA12 mutant polymerase (Fig. 5*A*), in contrast to observations made with WT Pol I (Fig. 2*D*). These data suggest that the A12 subunit may be necessary for the polymerase to sense the AT content of the downstream DNA and pause/arrest. Whether this sensory role is through direct contact with the DNA or through structural reorganization of the leading edge of the polymerase remains to be determined.

Structural data for Pol I and Pol II suggest that the trigger loop may also interact with the downstream DNA sequence (15, 33). To test whether the trigger loop of Pol I sensitizes the polymerase to downstream DNA sequence, we executed single-nucleotide addition transcription experiments with a Pol I trigger loop mutant to measure whether putative changes in trigger loop flexibility altered observed AT-dependent downstream sequence effects (Fig. 5*B*). These experiments were done with Pol I trigger loop mutant *rpa190-E1224G* (30, 37). This mutant has been shown to decrease the elongation rate in Pol I, and it has been hypothesized that this point mutation results in altered flexibility and dynamics of the trigger loop (30, 36, 37). In single-nucleotide addition time courses with E1224G Pol I on the high AT template, there was an increase in 10-mer species over the length of the time course (resulting in suppression of 11-mer species), but there was no significant change in the amplitude of CA dinucleotide produced (Fig. 2*E*). The lack of RNA cleavage suppression in single-nucleotide transcription by E1224G Pol I on the AT-rich template suggests that a polymerase with altered trigger loop flexibility may be insensitive to the +2 to +3 AT-rich region of the downstream DNA; thus, the

Downloaded from http://www.jbc.org/ at Univ of Alabama Birmingham, Lister Hill Library of the Health Sciences on April 24, 2020

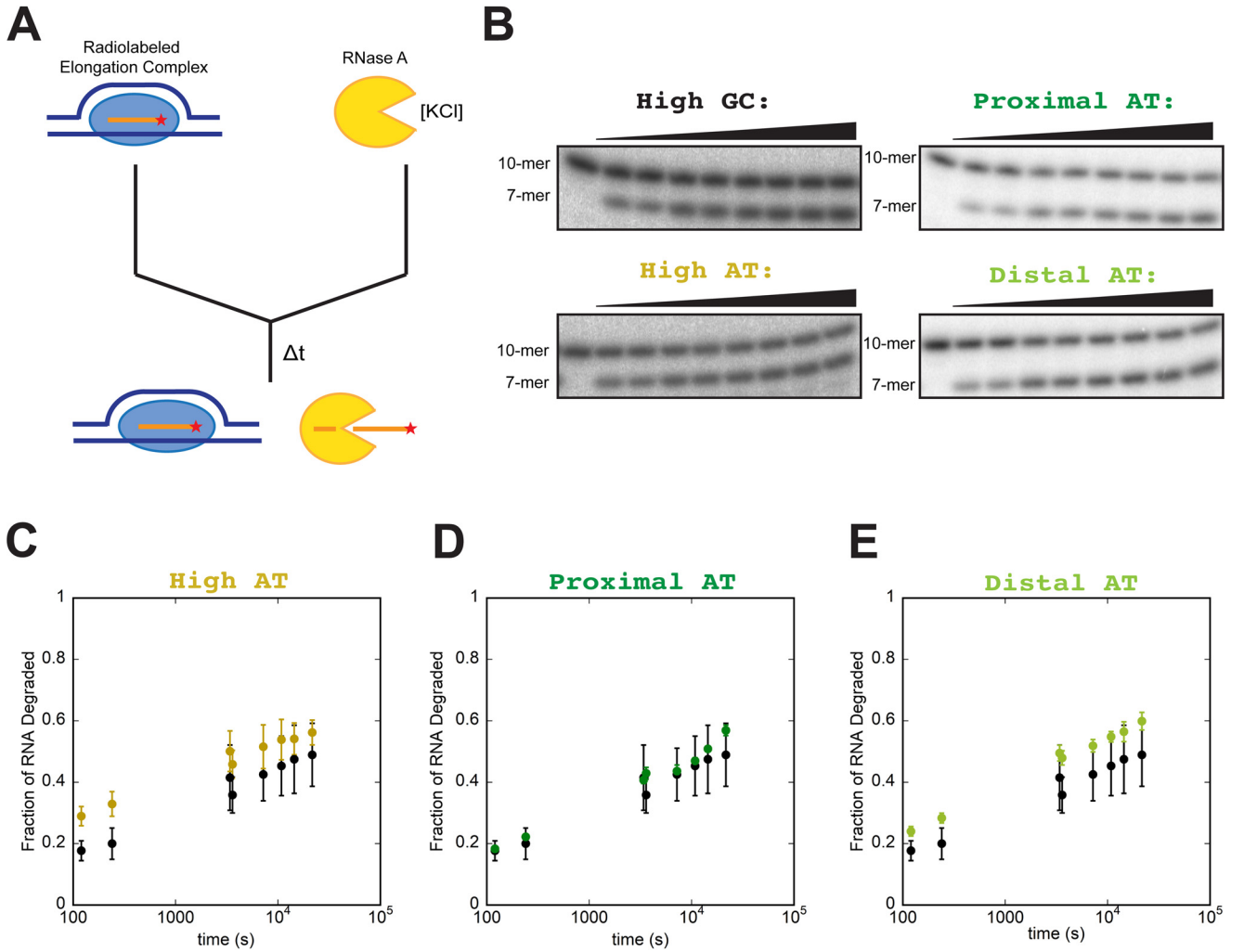

Figure 4. 11-mer suppression is not caused by destabilization of the elongation complex. *A*, schematic of the RNase elongation complex stability assay. The radiolabeled elongation complex is mixed with RNase A and allowed to incubate over time. Intact elongation complexes result in a 10-mer species, whereas disengaged elongation complexes result in free RNA that is rapidly cleaved by RNase A to a 7-mer species. *B*, representative time courses for high GC, high AT, proximal AT, and distal AT templates. *C–E*, quantification of elongation stability time courses for high AT (*C*, *gold*), proximal AT (*D*, *dark green*), distal AT (*E*, *light green*), and High GC (*C–E*, *black*) templates. Error bars represent standard deviation of the mean; $n = 3$ (*C–E*).

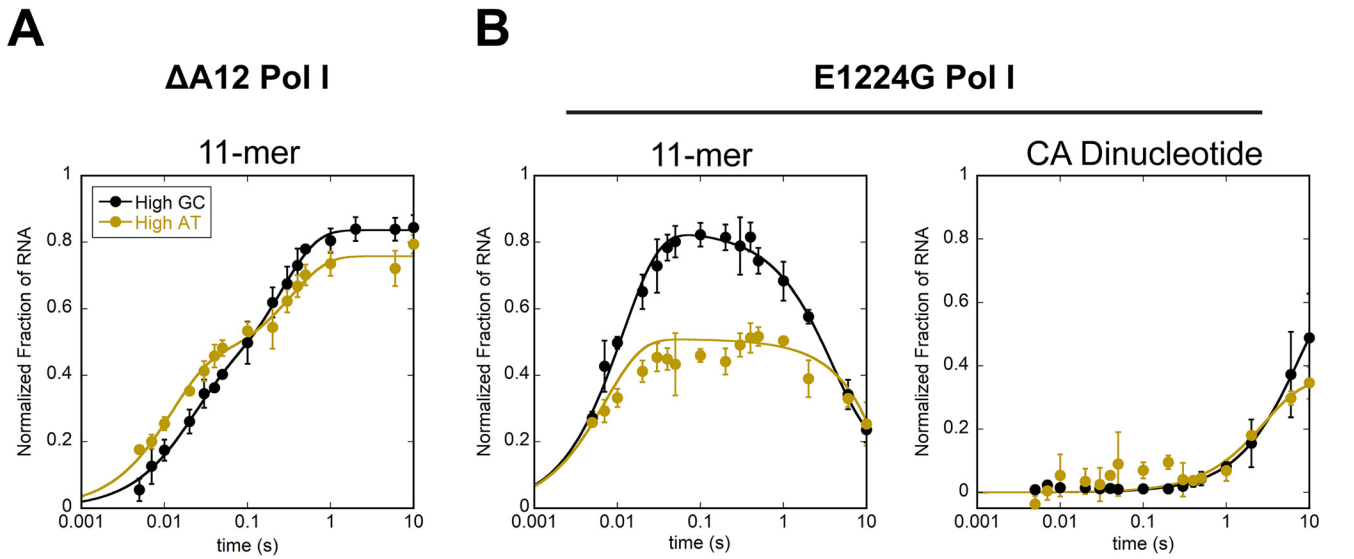

Figure 5. The A12 subunit and the trigger loop of Pol I sensitize the polymerase to the downstream DNA sequence. *A* and *B*, quantification of single-nucleotide addition time courses for ΔA12 Pol I (*A*) and E1224G Pol I (*B*). ΔA12 and E1224G 11-mer species were fit to the sum of two exponentials, whereas the E1224G CA dinucleotide species was fit to a single exponential. *Error bars* represent standard deviation of the mean. $n = 3$.

Downloaded from http://www.jbc.org/ at Univ of Alabama Birmingham, Lister Hill Library of the Health Sciences on April 24, 2020

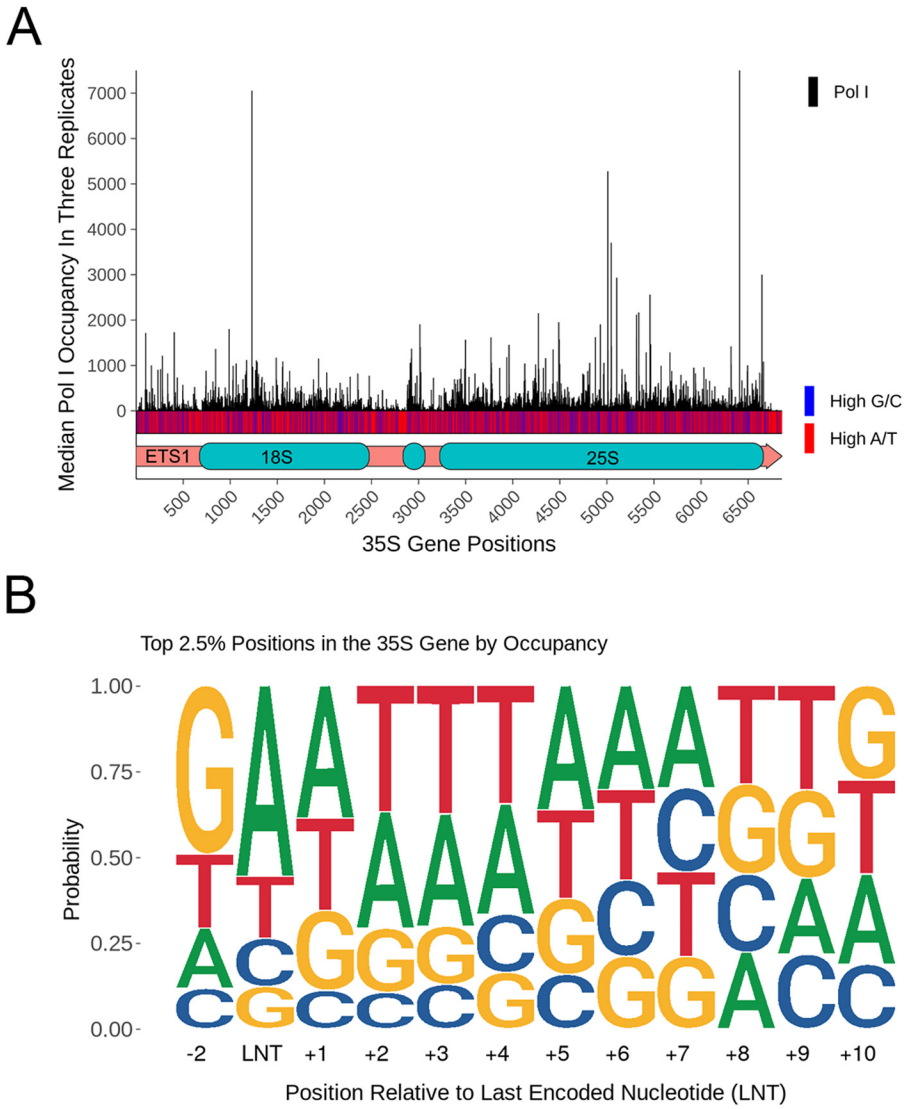

Figure 6. NET-seq reveals Pol I sensitivity to downstream sequence elements *in vivo*. *A*, line plot showing median Pol I occupancy in three biological replicates at each position within Pol I's only known transcriptional locus, the ^{35}S gene. Occupancy values are normalized to the sum of all occupancy in the Pol III–transcribed 5S gene (data not shown). Beneath the line plot is a heatmap displaying relative A/T and G/C nucleotide enrichment in 5-bp increments of the ^{35}S gene. *Blue* represents 0 A/T nucleotides in the 5-bp window (and, thus, five G/C nucleotides), and *red* indicates five A/T nucleotides in the 5-bp window (and, thus, no G/C residues). Beneath the heatmap is a diagram displaying the regions within the ^{35}S gene, with spacer regions shown in *salmon* and gene regions in *cyan*. *Left* to *right*: ETS 1, 18S, ITS 1 (not labeled), 5.8S (not labeled), ITS 2 (not labeled), 25S, and ETS 2 (not labeled). *B*, sequence logo generated from the top 2.5% of positions in the ^{35}S gene by Pol I occupancy.

trigger loop may directly or indirectly interact with this downstream DNA.

Analysis of NET-seq data reveals conservation of AT-rich downstream DNA effects in vivo

Although *in vitro* studies provide a detailed understanding of the potential impacts of downstream DNA sequence on polymerase activity, they do not assess *in vivo* impacts of these sequences. Our laboratory previously established NET-seq as a tool for quantifying relative Pol I occupancy *in vivo* in yeast (9). In brief, Pol I elongation complexes were immunoprecipitated from flash-frozen yeast cultures, and the nascent rRNA transcripts were isolated. The 3′ ends of these transcripts corresponded to the active site of their elongation complexes with single-nucleotide accuracy. The nascent RNAs were purified and used to generate libraries for next-generation sequencing. The reads from these libraries provided a cumulative snapshot of Pol I occupancy throughout the 35S ribosomal DNA gene (Fig. 6*A*). In the context of our *in vitro* findings, increased Pol I occupancy can be interpreted as increased dwell time before addition of subsequent nucleotides (consistent with amplitude suppression of the 11-mer species in our *in vitro* studies) or sequence-dependent backtracking and cleavage (consistent with dinucleotide production). NET-seq cannot differentiate between these two mechanistic explanations.

To determine whether there is a relationship between Pol I occupancy and downstream sequence, we first observed the downstream sequence content of the highest-occupancy positions. We then determined the top 2.5% of positions by occupancy (n = 172) for one replicate and compiled the sequences into a sequence logo (Fig. 6*B*). Within these positions, we observed a similar predominance of A and T residues in the last

Downloaded from http://www.jbc.org/ at Univ of Alabama Birmingham, Lister Hill Library of the Health Sciences on April 24, 2020

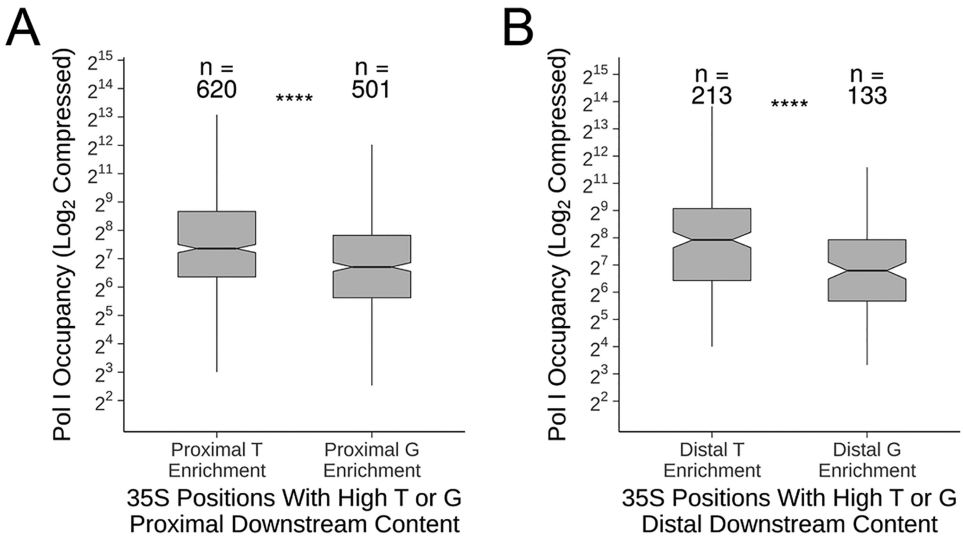

Figure 7. Proximal and distal nucleotide enrichment affect Pol I *in vivo*. *A*, notched boxplots of $\log_2$-compressed occupancy in ^{35}S positions with T or G residues proximally downstream (in positions +2 and +3). *B*, notched boxplots of ^{35}S positions with T or G residues distally downstream (positions +5 to +7). Each *box* represents the interquartile range for each enrichment group, with the *horizontal line* indicating the median value. The *notched portion* of each boxplot corresponds to the 95% confidence intervals for the median value. The *lower whisker* extends to the smallest observation greater than the lower quartile value minus the interquartile range multiplied by 1.5. The *upper whisker* extends to the largest observation smaller than the upper quartile value plus the interquartile range multiplied by 1.5 (51). Pol I occupancies in each region (see Fig. 5*A*, *diagram*) were normalized to the sum of occupancy in that region. Groups were compared by Wilcoxon rank-sum test. The number of observations in each enrichment group is listed above each boxplot, along with the *p* value for the Wilcoxon rank-sum test (****, $p < 5 \times 10^{-5}$).

encoded nucleotide position compared with the previous NET-seq study. Positions with G residue enrichment at the last encoded nucleotide also represent the minority within the top 2.5% position cohort, although not to the degree observed previously. The NET-seq libraries generated for this study have 10-fold greater read depth compared with the previous study, which may account for this difference (9). Strikingly, we observed a noted predominance of A and T residues directly downstream of these high-occupancy positions, suggesting that downstream A/T enrichment affects Pol I *in vivo* just as it does *in vitro* (Fig. 6). This enrichment was observed in the previous study, although it was not further investigated. This sequence enrichment was observed in all three replicates (Fig. S1). Next we sought to determine whether the exact sequences that were assayed *in vitro* above similarly affect Pol I *in vivo*. Unfortunately, there are not enough of these sequences within Pol I's limited transcriptome to support statistical analysis of the full high AT sequence (+2 to +3 concurrent with +5 to +7 high AT). Instead, we observed the effects of proximal (positions +2 to +3) and distal (positions +5 to +7) downstream enrichment of T and G residues on Pol I occupancy. We previously observed a systematic difference in occupancy between residues in gene regions (Fig. 6*A*, *cyan*) and spacer regions (Fig. 6*A*, *salmon*). To avoid bias between occupancy and gene region, the occupancy values in each region were normalized to the sum of occupancy within that region for the following analysis. We observed increased occupancy in positions with proximal downstream T residues relative to positions with proximal downstream G residues (Fig. 7*A*). Likewise, we observed increased occupancy in positions with distal T residue enrichment relative to those with distal G enrichment (Fig. 7*B*). Crucially, the difference between the distal enrichment groups was greater than between the proximal enrichment groups. These data suggest that distal T residue enrichment downstream affects Pol I *in vivo* just as it does *in vitro*, increasing dwell time prior to subsequent nucleotide addition steps. These trends held for all three replicates of our NET-seq data (Fig. S2).

To determine whether these phenomena occur gene-wide (as opposed to the smaller subsets shown in Fig. 7), the positions in the 35S ribosomal DNA gene were segregated by relative enrichment of each nucleotide in the +1 to +7 base-pair window downstream. Positions with high (four or greater) A (Fig. 8*A*) and T (Fig. 8*D*) enrichment in the 7-bp downstream window show significantly higher Pol I occupancy compared with positions with no A or T residues downstream, respectively. We observed the opposite trend for C and G nucleotides. Positions with any C (Fig. 8*B*) or G (Fig. 8*C*) nucleotides in their downstream DNA showed significantly decreased occupancy compared with positions with none (with the exception of the highest level of G enrichment). These trends were also observed in the other two replicates of our NET-seq data (Figs. S3 and S4). Collectively, these data show increased occupancy at positions with high A/T enrichment directly downstream and decreased occupancy at positions with high C/G enrichment directly downstream. These observations indicate that Pol I occupancy is affected by downstream sequence content *in vivo* just as it is *in vitro*. Although the difference between polymerase pausing and increased dwell time because of polymerase backtracking and cleavage cannot be distinguished in these data, either interpretation (or some combination of both) is in agreement with our *in vitro* findings.

Discussion

Downstream sequence impacts transcription elongation properties and elongation complex stability of RNA polymerase I

Significant effects on transcription complex pausing and dinucleotide production by Pol I occur in response to changes

Downloaded from http://www.jbc.org/ at Univ of Alabama Birmingham, Lister Hill Library of the Health Sciences on April 24, 2020

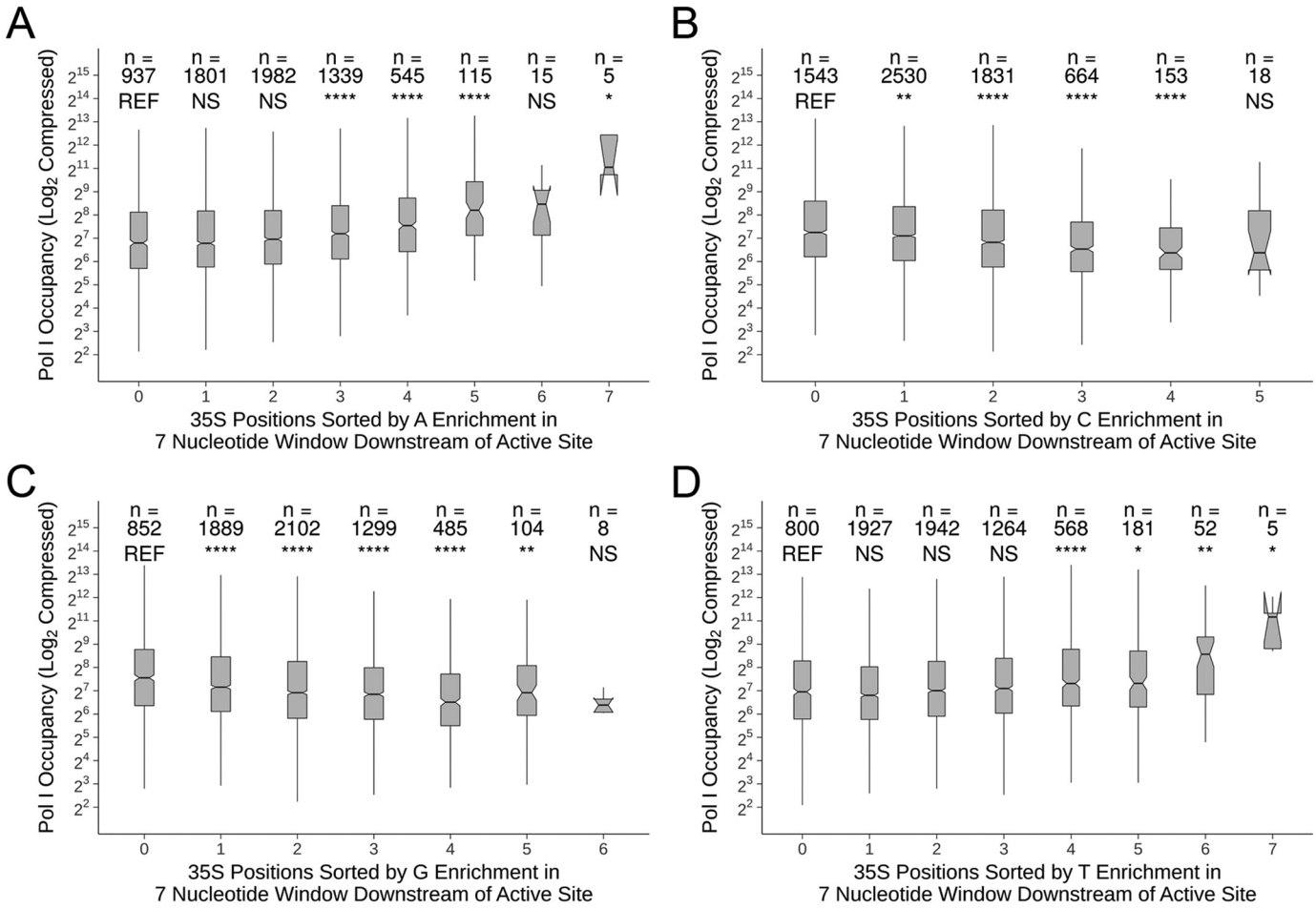

Figure 8. Downstream sequence enrichment for all four nucleotides affects Pol I occupancy. *A–D*, notched boxplots of $\log_2$-compressed Pol I occupancy in ^{35}S gene positions sorted by enrichment for A (*A*), C (*B*), G (*C*), and T (*D*) nucleotides in the 7-bp window directly downstream. Each *box* represents the interquartile range for each enrichment group, with the *horizontal line* indicating the median value. The notched portion of each boxplot corresponds to the 95% confidence intervals for the median value. The *lower whisker* extends to the smallest observation greater than the lower quartile value minus the interquartile range multiplied by 1.5. The *upper whisker* extends to the largest observation smaller than the upper quartile value plus the interquartile range multiplied by 1.5 (51). Each enrichment group is compared with the zero-residue enrichment group (reference group, *REF*) by Wilcoxon rank-sum test. The number of observations in each enrichment group is listed above each boxplot, along with the *p* value for the Wilcoxon rank-sum test. *ns*, not significant; *, $p < 5 \times 10^{-2}$; **, $p < 5 \times 10^{-3}$; ***, $p < 5 \times 10^{-4}$; ****, $p < 5 \times 10^{-5}$.

in downstream sequence both *in vivo* and *in vitro*. These effects (pausing/arrest and decreased RNA cleavage) correlate with sequences in distinct regions of the downstream sequence. G/C-to-A/T mutations revealed unique molecular consequences when introduced just downstream of the active site (proximal +2 to +3) *versus* distal mutation (+5 to +7). Downstream AT-dependent pausing has been observed previously in studies using human Pol II (15) and *E. coli* RNAP (17, 24) but never before for Pol I. Further, as Pol I carries its intrinsic cleavage factor as a *bona fide* subunit (the A12.2 subunit), this is the first record of AT-rich downstream DNA influence on nucleolytic cleavage. Collectively, these data suggest that downstream DNA has a significant impact on all stages of the transcription elongation cycle and that the polymerase itself interrogates the downstream DNA sequence.

Dependence on downstream sequence appears to be conserved among polymerases

Although *in vivo* studies have not yet revealed whether Pol II has similar responses to the downstream DNA sequence, it is clear that Pol I and II have similar responses to the content of downstream DNA *in vitro*. Previous literature has demonstrated that *E. coli* RNAP is likewise sensitive to downstream DNA sequence (17). A recent study of *E. coli* RNAP demonstrated that the DNA template sequence can result in elemental pausing where a subpopulation of polymerases exist in a half-translocated, backtracked state (80%), whereas a separate subpopulation of polymerases were capable of rapidly bypassing the pause state (20%) (24). These findings are strikingly similar to our observations here of a stably paused/arrested population of Pol I on the high AT template. These previously published *E. coli* RNAP data are further supported by structural data that demonstrated that elemental paused elongation complexes can (but do not always) result in a distinct tilted rearrangement of the RNA:DNA hybrid (24, 38). Our laboratory has demonstrated previously that, on the high GC template in single-nucleotide addition experiments, the chemical step is rate-limiting, substantiated by the observed coupling of [ATP] to the chemical step and by Pol I's sensitivity to a slowly hydrolysable nucleotide analog (Sp-ATPαS) (30, 31). However, model-de-

Downloaded from http://www.jbc.org/ at Univ of Alabama Birmingham, Lister Hill Library of the Health Sciences on April 24, 2020

pendent fitting of single-nucleotide transcription experiments requires inclusion of a transient state of polymerases (~20%) that slowly (relative to ATP binding and the chemical step) transitions into an active state (31, 32). This Pol I population exists prior to nucleotide binding, and in our experimental strategy, we were insensitive to the translocation state of this slow population of polymerases. Further structural studies of the Pol I elongation complex on templates with varying downstream sequences could further elucidate the physical nature of the observed slow population of kinetically paused polymerases.

Previous work by Landick and co-workers (15) showed that that AT-rich downstream DNA results in an increase in stable pause and arrest by human Pol II compared with DNA with greater GC content. In that study, Palangat et al. (15) found that Pol II is likewise specifically sensitive to downstream AT sequences based on the proximity of the AT-rich DNA to the active site. They noted that changes in DNA flexibility and torsion were not responsible for these observations. They further hypothesized that interactions with the trigger loop domain of Pol II were likely responsible to sensitivities in downstream DNA (15). Although we did not observe changes in polymerase pausing with AT-rich downstream DNA with the E1224G Pol I trigger loop mutant, it is possible that the phenotype induced by E1224G on Pol I activity is not severe enough to elicit a change in downstream DNA sensitivity.

Potential interactions between the Pol I trigger loop, the A12 subunit, and downstream DNA

Landick and co-workers (15) altered downstream AT content for human Pol II and observed effects on elongation complex stability, pausing, and arrest with AT-rich downstream DNA. They analyzed structural data for human Pol II and hypothesized that the downstream DNA may be sensed by the trigger loop domain (15). Our laboratory observed that alterations in trigger loop residues in Pol I have an opposite effect when compared with their Pol II counterparts. Nevertheless, we used this well-described Pol I trigger loop mutant to interrogate whether alteration of trigger loop flexibility would result in changes in sensitivity to AT-rich downstream DNA. We observed that E1224G Pol I on the high AT template did exhibit some recovery of dinucleotide cleavage, but the amplitude of the 11-mer species was still suppressed. This observation suggests that the trigger loop of Pol I may be responsible for partially sensitizing the polymerase to the downstream DNA sequence or that the dynamic nature of this domain is considerably different in Pol I compared with Pol II.

Because of the A12 subunit's role in backtracking, termination, and cleavage (35, 39, 40), it stood to reason that A12 could contribute to interactions between the polymerase and the downstream DNA. When we compared ΔA12 Pol I transcription elongation time courses on the high GC and high AT sequences, we observed subtle changes in transcription elongation kinetics. A12 contributes to a number of enzymatic properties of Pol I, including nucleotide addition, dinucleotide cleavage, and backtracking (32, 34, 35). Rpa12 is also thought to stabilize the association of subunits A49 and A34.5 to Pol I (40). Because the A12 subunit is involved in such a wide array of activities, it is impossible to dissect whether these effects are a result of direct contact with A12 or due to indirect effects on the conformational dynamics of other subunits. However, these data do suggest that A12 is at least in part responsible for sensitization of the polymerase to the downstream DNA. Further characterization of the roles of A34.5/A49 and the C terminus of the A12 subunit will identify individual contributions of these subunits to Pol I pausing and backtracking. Future structural studies may identify the physical nature of the interaction between A12 and the downstream DNA.

Implications of polymerase sensitivity to downstream DNA

It is now clear that polymerases from prokaryotes to eukaryotes display sensitivity to downstream DNA sequence and that this sensitivity has impacts on the entirety of the transcription cycle. It has been known for decades that transcription termination is controlled by DNA/RNA sequence (9). It is reasonable that transcription elongation may be similarly controlled by DNA/RNA sequence. The role of downstream DNA sequence in transcription elongation is important because the elongation rate directly affects overall gene expression by *E. coli* RNAP, splicing by eukaryotic Pol II, and ribosome biogenesis by eukaryotic Pol I (2). Here we demonstrate that downstream DNA sequence does, in fact, impact all stages of the transcription elongation cycle. Further, sensitivities to particular regions of downstream DNA appear to be conserved between eukaryotic Pol I and Pol II (15). This sensitivity is conserved *in vivo*, suggesting that downstream DNA sequence can directly impact Pol I-mediated rRNA biogenesis. This sensitivity to downstream DNA could function as a "second code" and directly govern the efficiency of RNA processing, thus having large-scale impacts on global gene expression.

Experimental procedures

Yeast strains, media, and growth conditions

Yeast strains containing *rpa190-E1224G* Pol I, *rpa12*Δ Pol I, and WT Pol I have been described previously (9, 34, 37).

Protein purification

rpa190-E1224G Pol I, *rpa12*Δ Pol I, and WT Pol I were purified exactly as described previously (34, 37, 41). Briefly, 50 liters of yeast cells were grown to late log phase (when cell growth begins to slow). Cells were harvested by centrifugation and frozen. Cells were thawed and lysed in breakage buffer (400 mM ammonium sulfate, 100 mM Tris-sulfate (pH 7.9) at 4 °C, 20% (v/v) glycerol, 5 mM $MgCl_2$ 5 mM imidazole, 1 mM PMSF, and 0.1% (v/v) Tween 20), and endogenously His-tagged proteins were sequentially purified using a Ni Sepharose 6 Fast Flow column (GE Healthcare) and a HiTrap Heparin HP column (GE Healthcare) followed by a MonoQ 5/50 GL column (GE Healthcare). Proteins were aliquoted and stored in storage buffer (monoQ elution buffer supplemented with 40% glycerol) at −80 °C.

Single-nucleotide in vitro transcription

Single nucleotide addition assays for Pol I and the Pol I mutants *rpa190-E1224G* and ΔA12 were performed as de-

Downloaded from http://www.jbc.org/ at Univ of Alabama Birmingham, Lister Hill Library of the Health Sciences on April 24, 2020

scribed previously (31). Briefly, Pol I elongation complexes were preformed in a synthetic elongation complex with 54 nM template DNA prehybridized to 163 nM RNA and 163 nM non-template DNA in 40 mM KCl, 20 mM Tris-OAc (pH 7.9 at 25 °C), 0.2 mg/ml BSA, and 2 mM DTT. Elongation complexes were radioactively labeled for 10 min with 5 nM [α-^{32}P]CTP in 100 μM $Mg(OAc)_2$, 40 mM KCl, and 20 mM Tris-OAc (pH 7.9 at 25 °C). Labeling was quenched by mixing with 1.1 mM EDTA-K_3 and 5 μM CTP in 40 mM KCl and 20 mM Tris-OAc (pH 7.9 at 25 °C). Labeled elongation complexes were then mixed in a chemically quenched flow over a series of time points with a 2× concentration ATP substrate mixture containing 2 mM ATP, 0.1 mg/ml heparin, and 18 mM $Mg(OAc)_2$ in 1× concentration 0.2 mg/ml BSA, 2 mM DTT, 40 mM KCl, and 20 mM Tris-OAc (pH 7.9 at 25 °C).

NET-seq library preparation

Three NET-seq libraries were prepared with an *S. cerevisiae* strain bearing a C-terminal triple HA (3×HA, His_7) tag on the A135 subunit of Pol I as described previously (9). NET-seq read trimming and alignment to the *S. cerevisiae* genome were performed as described previously (9). Unix Scripts are available upon request.

Net-seq analysis

For Fig. 6*A*, Pol I occupancy on the negative strand in the 35S ribosomal DNA gene was normalized to the sum of counts on the positive strand of the 5S gene for each replicate and multiplied by 1,000. The median occupancy value from the three replicates for each position is displayed in Fig. 6*A*, *top panel*. The heat map in Fig. 6*A* (directly below the median occupancy plot) was created by determining the enrichment of A/T residues in five-residue increments throughout the 35S ribosomal DNA gene. These windows were then color-coded according to relative A/T enrichment: *blue* for 0 A/T residues and *red* for 5 A/T residues.

For Fig. 8, Pol I occupancy on the negative strand in each region (ETS 1, 18S, ITS 1, 5.8S, ITS 2, 25S, and the first 91 bp of ETS 2) of the ^{35}S gene was normalized to the sum of counts in that region and multiplied by 1,000,000 to account for previously observed region-specific variations in median occupancy (9). Positions were segregated according to enrichment for each nucleotide in the 7-bp window directly downstream (positions +1 to +7). The upper and lower 95% confidence intervals for the median value (corresponding to the upper and lower bounds of the notched portion in each boxplot) were equal to the median value ± (1.58 × IQR/($\sqrt{}$n), where IQR is the interquartile range and n is the number of observations in each group. Each level of nucleotide enrichment was compared via Wilcoxon rank-sum test to the lowest level of nucleotide enrichment (0 residues). Pol I occupancies were $\log_2$-compressed (using the formula $y = \log_2(x + 1)$) for ease of *y* axis visualization. Displayed data (Fig. 8) are from one representative replicate. Analyses and figure generation were performed using R version 3.4.2 (42) using the following packages: dplyr version 0.7.5 (43), plyr version 1.4.2 (44), ggplot2 version 2.2.1 (45), ggpubr version 0.1.7 (46), cowplot version 0.9.2 (47), devtools version 2.0.1 (48), matrixStats version 0.53.1 (49), and metaMA version 3.1.2 (50). R scripts are available upon request.

Author contributions—C. E. S., A. L. L., and D. A. S. conceptualization; C. E. S., A. M. C., and D. A. S. data curation; C. E. S., A. M. C., A. L. L., and D. A. S. formal analysis; C. E. S. and A. M. C. validation; C. E. S. and A. M. C. investigation; C. E. S. and A. M. C. visualization; C. E. S. and A. M. C. methodology; C. E. S. writing-original draft; C. E. S., A. M. C., A. L. L., and D. A. S. writing-review and editing; A. L. L. and D. A. S. project administration; D. A. S. supervision; D. A. S. funding acquisition.

Acknowledgments—We thank the members of the Lucius and Schneider laboratories for helpful advice and critical evaluation of this work.

References

1. Jonkers, I., Kwak, H., and Lis, J. T. (2014) Genome-wide dynamics of Pol II elongation and its interplay with promoter proximal pausing, chromatin, and exons. *eLife* **3,** e02407 CrossRef Medline
2. Scull, C. E., and Schneider, D. A. (2019) Coordinated control of rRNA processing by RNA polymerase I. *Trends Genet.* **35,** P724–P733 CrossRef Medline
3. Hodges, C., Bintu, L., Lubkowska, L., Kashlev, M., and Bustamante, C. (2009) Nucleosomal fluctuations govern the transcription dynamics of RNA polymerase II. *Science* **325,** 626–628 CrossRef Medline
4. Renner, D. B., Yamaguchi, Y., Wada, T., Handa, H., and Price, D. H. (2001) A highly purified RNA polymerase II elongation control system. *J. Biol. Chem.* **276,** 42601–42609 CrossRef Medline
5. Peterlin, B. M., and Price, D. H. (2006) Controlling the elongation phase of transcription with P-TEFb. *Mol. Cell* **23,** 297–305 CrossRef Medline
6. Gabizon, R., Lee, A., Vahedian-Movahed, H., Ebright, R. H., and Bustamante, C. J. (2018) Pause sequences facilitate entry into long-lived paused states by reducing RNA polymerase transcription rates. *Nat. Commun.* **9,** 2930 CrossRef Medline
7. Tadigotla, V. R., O Maoiléidigh, D., Sengupta, A. M., Epshtein, V., Ebright, R. H., Nudler, E., and Ruckenstein, A. E. (2006) Thermodynamic and kinetic modeling of transcriptional pausing. *Proc. Natl. Acad. Sci. U.S.A.* **103,** 4439–4444 CrossRef Medline
8. Czyz, A., Mooney, R. A., Iaconi, A., and Landick, R. (2014) Mycobacterial RNA polymerase requires a U-Tract at intrinsic terminators and is aided by NusG at suboptimal terminators. *mBio* **5,** e00931 CrossRef Medline
9. Clarke, A. M., Engel, K. L., Giles, K. E., Petit, C. M., and Schneider, D. A. (2018) NETSeq reveals heterogeneous nucleotide incorporation by RNA polymerase I. *Proc. Natl. Acad. Sci. U.S.A.* **115,** E11633–E11641 CrossRef Medline
10. Vvedenskaya, I. O., Vahedian-Movahed, H., Bird, J. G., Knoblauch, J. G., Goldman, S. R., Zhang, Y., Ebright, R. H., and Nickels, B. E. (2014) Interactions between RNA polymerase and the "core recognition element" counteract pausing. *Science* **344,** 1285–1289 CrossRef Medline
11. Hein, P. P., Palangat, M., and Landick, R. (2011) RNA transcript 3′-proximal sequence affects translocation bias of RNA polymerase. *Biochemistry* **50,** 7002–7014 CrossRef Medline
12. Cabrera-Ostertag, I. J., Cavanagh, A. T., and Wassarman, K. M. (2013) Initiating nucleotide identity determines efficiency of RNA synthesis from 6S RNA templates in *Bacillus subtilis* but not *Escherichia coli*. *Nucleic Acids Res.* **41,** 7501–7511 CrossRef Medline
13. Helmann, J. D. (1995) Compilation and analysis of *Bacillus subtilis* σ A-dependent promoter sequences: evidence for extended contact between RNA polymerase and upstream promoter DNA. *Nucleic Acids Res.* **23,** 2351–2360 CrossRef Medline
14. Holmes, S. F., and Erie, D. A. (2003) Downstream DNA sequence effects on transcription elongation: allosteric binding of nucleoside triphosphates facilitates translocation via a ratchet motion. *J. Biol. Chem.* **278,** 35597–35608 CrossRef Medline

Downloaded from http://www.jbc.org/ at Univ of Alabama Birmingham, Lister Hill Library of the Health Sciences on April 24, 2020

ASBMB

15. Palangat, M., Hittinger, C. T., and Landick, R. (2004) Downstream DNA selectively affects a paused conformation of human RNA polymerase II. *J. Mol. Biol.* **341,** 429–442 CrossRef Medline
16. Nudler, E., Avetissova, E., Markovtsov, V., and Goldfarb, A. (1996) Transcription processivity: protein-DNA interactions holding together the elongation complex. *Science* **273,** 211–217 CrossRef Medline
17. Lee, D. N., Phung, L., Stewart, J., and Landick, R. (1990) Transcription pausing by *Escherichia coli* RNA polymerase is modulated by downstream DNA sequences. *J. Biol. Chem.* **265,** 15145–15153 Medline
18. Ederth, J., Artsimovitch, I., Isaksson, L. A., and Landick, R. (2002) The downstream DNA jaw of bacterial RNA polymerase facilitates both transcriptional initiation and pausing. *J. Biol. Chem.* **277,** 37456–37463 CrossRef Medline
19. Ederth, J., Mooney, R. A., Isaksson, L. A., and Landick, R. (2006) Functional interplay between the jaw domain of bacterial RNA polymerase and allele-specific residues in the product RNA-binding pocket. *J. Mol. Biol.* **356,** 1163–1179 CrossRef Medline
20. Kyzer, S., Ha, K. S., Landick, R., and Palangat, M. (2007) Direct versus limited-step reconstitution reveals key features of an RNA hairpin-stabilized paused transcription complex. *J. Biol. Chem.* **282,** 19020–19028 CrossRef Medline
21. Windgassen, T. A., Mooney, R. A., Nayak, D., Palangat, M., Zhang, J., and Landick, R. (2014) Trigger-helix folding pathway and SI3 mediate catalysis and hairpin-stabilized pausing by *Escherichia coli* RNA polymerase. *Nucleic Acids Res.* **42,** 12707–12721 CrossRef Medline
22. Larson, M. H., Zhou, J., Kaplan, C. D., Palangat, M., Kornberg, R. D., Landick, R., and Block, S. M. (2012) Trigger loop dynamics mediate the balance between the transcriptional fidelity and speed of RNA polymerase II. *Proc. Natl. Acad. Sci. U.S.A.* **109,** 6555–6560 CrossRef Medline
23. Larson, M. H., Mooney, R. A., Peters, J. M., Windgassen, T., Nayak, D., Gross, C. A., Block, S. M., Greenleaf, W. J., Landick, R., and Weissman, J. S. (2014) A pause sequence enriched at translation start sites drives transcription dynamics *in vivo*. *Science* **344,** 1042–1047 CrossRef Medline
24. Saba, J., Chua, X. Y., Mishanina, T. V., Nayak, D., Windgassen, T. A., Mooney, R. A., and Landick, R. (2019) The elemental mechanism of transcriptional pausing. *eLife* **8,** e40981 CrossRef Medline
25. Schneider, D. A., French, S. L., Osheim, Y. N., Bailey, A. O., Vu, L., Dodd, J., Yates, J. R., Beyer, A. L., and Nomura, M. (2006) RNA polymerase II elongation factors Spt4p and Spt5p play roles in transcription elongation by RNA polymerase I and rRNA processing. *Proc. Natl. Acad. Sci. U.S.A.* **103,** 12707–12712 CrossRef Medline
26. Schneider, D. A., Michel, A., Sikes, M. L., Vu, L., Dodd, J. A., Salgia, S., Osheim, Y. N., Beyer, A. L., and Nomura, M. (2007) Transcription elongation by RNA polymerase I is linked to efficient rRNA processing and ribosome assembly. *Mol. Cell* **26,** 217–229 CrossRef Medline
27. Mills, E. W., and Green, R. (2017) Ribosomopathies: there's strength in numbers. *Science* **358,** eaan2755 CrossRef Medline
28. Hannan, R. D., Drygin, D., and Pearson, R. B. (2013) Targeting RNA polymerase I transcription and the nucleolus for cancer therapy. *Expert Opin. Ther. Targets* **17,** 873–878 CrossRef Medline
29. Scull, C. E., Zhang, Y., Tower, N., Rasmussen, L., Padmalayam, I., Hunter, R., Zhai, L., Bostwick, R., and Schneider, D. A. (2019) Discovery of novel inhibitors of ribosome biogenesis by innovative high throughput screening strategies. *Biochem. J.* **476,** 2209–2219 CrossRef Medline
30. Scull, C. E., Ingram, Z. M., Lucius, A. L., and Schneider, D. A. (2019) A novel assay for RNA polymerase I transcription elongation sheds light on the evolutionary divergence of eukaryotic RNA polymerases. *Biochemistry* **58,** 2116–2124 CrossRef Medline
31. Appling, F. D., Lucius, A. L., and Schneider, D. A. (2015) Transient-state kinetic analysis of the RNA polymerase I nucleotide incorporation mechanism. *Biophys. J.* **109,** 2382–2393 CrossRef Medline
32. Appling, F. D., Schneider, D. A., and Lucius, A. L. (2017) Multisubunit RNA polymerase cleavage factors modulate the kinetics and energetics of nucleotide incorporation: an RNA polymerase I case study. *Biochemistry* **56,** 5654–5662 CrossRef Medline
33. Tafur, L., Sadian, Y., Hoffmann, N. A., Jakobi, A. J., Wetzel, R., Hagen, W. J. H., Sachse, C., and Müller, C. W. (2016) Molecular structures of transcribing RNA polymerase I. *Mol. Cell* **64,** 1135–1143 CrossRef Medline
34. Appling, F. D., Scull, C. E., Lucius, A. L., and Schneider, D. A. (2018) The A12.2 subunit is an intrinsic destabilizer of the RNA polymerase I elongation complex. *Biophys. J.* **114,** 2507–2515 CrossRef Medline
35. Lisica, A., Engel, C., Jahnel, M., Roldán, É., Galburt, E. A., Cramer, P., and Grill, S. W. (2016) Mechanisms of backtrack recovery by RNA polymerases I and II. *Proc. Natl. Acad. Sci. U.S.A.* **113,** 2946–2951 CrossRef Medline
36. Kireeva, M. L., Nedialkov, Y. A., Cremona, G. H., Purtov, Y. A., Lubkowska, L., Malagon, F., Burton, Z. F., Strathern, J. N., and Kashlev, M. (2008) Transient reversal of RNA polymerase II active site closing controls fidelity of transcription elongation. *Mol. Cell* **30,** 557–566 CrossRef Medline
37. Viktorovskaya, O. V., Engel, K. L., French, S. L., Cui, P., Vandeventer, P. J., Pavlovic, E. M., Beyer, A. L., Kaplan, C. D., and Schneider, D. A. (2013) Divergent contributions of conserved active site residues to transcription by eukaryotic RNA polymerases I and II. *Cell Rep.* **4,** 974–984 CrossRef Medline
38. Kang, J. Y., Mishanina, T. V., Bellecourt, M. J., Mooney, R. A., Darst, S. A., and Landick, R. (2018) RNA polymerase accommodates a pause RNA hairpin by global conformational rearrangements that prolong pausing. *Mol. Cell* **69,** 802–815.e5 CrossRef Medline
39. Prescott, E. M., Osheim, Y. N., Jones, H. S., Alen, C. M., Roan, J. G., Reeder, R. H., Beyer, A. L., and Proudfoot, N. J. (2004) Transcriptional termination by RNA polymerase I requires the small subunit Rpa12p. *Proc. Natl. Acad. Sci. U.S.A.* **101,** 6068–6073 CrossRef Medline
40. Tafur, L., Sadian, Y., Hanske, J., Wetzel, R., Weis, F., and Müller, C. W. (2019) The cryo-EM structure of a 12-subunit variant of RNA polymerase I reveals dissociation of the A49-A34.5 heterodimer and rearrangement of subunit A12.2. *eLife* **8,** e43204 CrossRef Medline
41. Schneider, D. A. (2012) Quantitative analysis of transcription elongation by RNA polymerase I *in vitro*. *Methods Mol. Biol.* **809,** 579–591 CrossRef Medline
42. R Development Core Team (2013) *R: A Language and Environment for Statistical Computing* (R Foundation for Statistical Computing).
43. Wickham, H., Francois, R., Henry, L., and Müller, K. (2018) *dplyr: A Grammar of Data Manipulation*, R Package Version 0.7.6
44. Wickham, H. (2011) The split-apply-combine strategy for data analysis. *Journal of Statistical Software* **40,** 1–29
45. Wickham, H. (2016) *ggplot2: elegant graphics for data analysis*, Springer
46. Kassambara, A. (2017) ggpubr: "ggplot2" based publication ready plots (version 0.1. 7).
47. Wilke, C. (2017). *Cowplot: Streamlined Plot Theme and Plot Annotations for "ggplot2'," R* Package Version 0.9. 2
48. Wickham, H., and Chang, W. (2019) *devtools: Tools to Make Developing R Packages Easier*. 2016. R Package Version 1, 381
49. Bengtsson, H. (2017) *matrixStats: Functions that Apply to Rows and Columns of Matrices (and to Vectors). CRAN R package*
50. Marot, G., Foulley, J.-L., Mayer, C.-D., and Jaffrézic, F. (2009) Moderated effect size and *p*-value combinations for microarray meta-analyses. *Bioinformatics* **25,** 2692–2699 CrossRef Medline
51. McGill, R., Tukey, J. W., and Larsen, W. A. (1978) Variations of box plots. *The American Statistician* **32,** 12–16

Downloaded from http://www.jbc.org/ at Univ of Alabama Birmingham, Lister Hill Library of the Health Sciences on April 24, 2020

Downstream sequence-dependent RNA cleavage and pausing by RNA polymerase I

Catherine E. Scull, Andrew M. Clarke, Aaron L. Lucius and David Alan Schneider

J. Biol. Chem. 2020, 295:1288-1299.
doi: 10.1074/jbc.RA119.011354 originally published online December 16, 2019

Access the most updated version of this article at doi: 10.1074/jbc.RA119.011354

Alerts:
- When this article is cited
- When a correction for this article is posted

Click here to choose from all of JBC's e-mail alerts

This article cites 44 references, 17 of which can be accessed free at
http://www.jbc.org/content/295/5/1288.full.html#ref-list-1

Downloaded from http://www.jbc.org/ at Univ of Alabama Birmingham, Lister Hill Library of the Health Sciences on April 24, 2020